IET Nanobiotechnology

Research Article

IET Journals
The Institution of Engineering and Technology

Method for enhancing bioavailability of myricetin based on self-assembly of casein–myricetin nanomicelles

ISSN 1751-8741
Received on 19th December 2018
Revised 12th October 2019
Accepted on 31st January 2020
E-First on 27th February 2020
doi: 10.1049/iet-nbt.2018.5431
www.ietdl.org

Hui Guo[1] ✉, Yun Fei Chen[1], Yi Tang[1], Jun Qing Qian[1]

[1]*College of Pharmaceutical Science, Zhejiang University of Technology, Hangzhou 310014, People's Republic of China*

✉ *E-mail: tggh635@163.com*

Abstract: In order to expand the application in the medical field and enhance pharmacological effects, casein–myricetin nanomicelles were prepared by the self-assembly method and characterised by ultraviolet–visible spectroscopy and Fourier transform infrared spectroscopy. The parameters in self-assembly were optimised according to the factors of particle size, encapsulation yield, and drug loading. The result showed a pH of 5.5, a casein concentration of 2 mg/ml, a mass ratio of casein to myricetin of 8:1, ultrasonic power of 300 W, ultrasonic time of 5 min and ethanol volume of 7 ml were the optimal conditions. The situ cycle intestinal perfusion methods indicated that casein–myricetin nanomicelles can be more easily absorbed by small intestine than myricetin standard sample. Therefore, casein micelles are effective for improving the water solubility of myricetin.

1 Introduction

Myricetin is commonly found in the leaves, cortex, and roots of the waxberry, which also can be detected micro-amounts in tea. The extensive biological activities of myricentin have been reported, such as antibacterial, antiviral, hypoglycaemic effect, anti-tumour [1], neuroprotective [2], anti-inflammatory [3, 4], antioxidation and liver protection [5]. However, its application in pharmaceutical industries is limited at present because of its high hydrophobicity, poor stability in specific environments (temperature, light, and oxygen) [6], and poorly bioavailable [7]. Therefore, it is very important to develop a preparation, which can improve bioavailability and prolong the time of bioactivity. A variety of delivery vehicles, including liposomes, microemulsions, and cyclodextrin clathrate compounds have been previously developed. Landi-Librandi *et al*. [8] found myricetin liposomes had a significant improvement in antioxidant activity and membrane permeability. Myricetin oil/water micro-emulsion prepared by Zhang *et al*. [9] has greatly increased the water solubility and controlled-release effect of the drug properties. Myricetin–hydroxypropyl-β-cyclodextrin complex was studied by Yao *et al*. [10], and the results showed that the water solubility, dissolution rate, and oral bioavailability of myricetin were greatly enhanced. However, these methods have some limitations such as poor stability and toxicity. It has been confirmed that the binding of flavonoids with proteins may be helpful to the pharmacodynamics [11]. As a novel method of drug structure modification, self-assembly can improve drug performance. In particular, some protein macromolecular compounds have become a research hotspot in the field of self-assembly due to their non-immunogenicity, good biodegradability, biocompatibility, safety, and non-toxicity [12–14].

Molecular self-assembly is the spontaneous organisation of molecules under thermodynamic equilibrium conditions into the structurally well-defined and rather stable arrangement through a number of non-covalent interactions [15, 16]. This self-assembly process mainly relies on van der Waals forces, hydrogen bonds, electrostatic forces, and coordination bonds, forming ordered, stable and intact analytical structure of self-assembly system [17]. The materials used for molecules self-assembly are mostly amphiphilic materials, of which the protein is the most studied [18, 19].

Casein is a good material for encapsulating nutrients that can form spherical clusters of several hundred nanometres in diameter by self-assembly in aqueous solution. Casein is a major protein in milk (about 80% of the protein) and represents a family of four gene products (s1-, s2-, α-, and β-casein) [20]. Being a dietary protein, casein possesses biodegradability and biocompatibility on oral administration [21]. These four kinds of proteins are chain amphiphilic proteins with hydrophobic and hydrophilic regions. The hydrophobic part can self-assemble as micelles and bind myricetin to increase the solubility in water and improve the bioavailability, which provides a broad prospect for further improving the development and utilisation of myricetin. Casein micelles diameter ranges from 80 to 400 nm, and the average diameter was 200 nm [22]. Compared with other delivery vehicles, casein self-assembly has the following advantages: firstly, low toxicity and high safety; secondly, the prepared nanomicelles have high stability and targeted delivery of active ingredients in the inner environment; thirdly, nanomicelles can prolong the residence time of the carrier and promote the absorption of drugs [23]. Therefore, casein micelles can be exploited as a natural delivery vehicle for various hydrophobic compounds such as quercetin [24], eriocitrin [25], curcumin [26, 27], Glimepiride [28], (−)-epigallocatechin gallate [29].

Accordingly, the objective of this study is to prepare casein–myricetin nanomicelles to improve the bioavailability of myricetin. The encapsulation capability of the casein particle and the influence of various factors were studied to determine the optimal process condition.

2 Materials and methods

2.1 Materials

Casein (cp, nitrogen content of 14.5–15.5%) and phenolsulphonphthalein (PSP) were purchased from Sinopharm Chemical Reagent Co., Ltd. Hydrochloric acid, sodium hydroxide, and anhydrous ethanol were purchased from Ante Biochem Co., Ltd (Anhui, China). 98% myricetin was purchased from Dekang Biological Co., Ltd (Ningbo, China). Stroke-physiological saline solution, Krebs–Ringer phosphate (homemade), chloral hydrate was from Aladdin Biochemical Technology Co., Ltd (Shanghai, China), and other chemicals were of analytical grade. Sprague–Dawley (SD) rats (weight 200 ± 20 g) were obtained from the Animal Center of Zhejiang Academy of Medical Sciences (Zhejiang, China).

2.2 Instrumentation

The diameter of particles was measured by nanoparticle size analyser (Nano-S9, Malvern Instruments Ltd, UK). High performance liquid chromatography (HPLC; Agilent 1200, Agilent Technologies Inc.) was used to determine the myricetin concentration. Sample absorbance was measured by using an ultraviolet (UV) spectrophotometer (752, Shanghai Spectrum Instrument). The structure of myricetin–casein serum albumin nanomicelles was characterised by using an infrared spectrometer (AVATAR370, Thermo Nicolet Corporation, USA).

2.3 Preparation of myricetin–casein nanomicelles

Myricetin–casein nanomicelles were prepared following the reported method with some modifications [30]. Briefly, an amount of casein was dissolved in 50 ml of sodium hydroxide solution, stirred under 30°C and pH was adjusted. Also, a certain quantity of myricetin was dissolved in 5 ml ethanol. The above solutions were mixed and sonicated for 5 min. The obtained solution was evaporated to remove ethanol and centrifuged at 4000 rpm for 10 min, and then the supernatant was concentrated and freeze-dried to obtain casein–myricetin nanomicelles.

2.4 Encapsulation yield and drug loading

Casein–myricetin nanomicelles (1 ml) were diluted to 10 ml and sonicated 5 min so that the myricetin encapsulated in casein is completely released into the solution, and detected the myricetin concentration by HPLC. The encapsulation yield and drug loading are calculated as shown in (1) and (2), respectively

$$\text{Encapsulation} = \frac{C \times V}{m \times 10^6} \times 100\% \quad (1)$$

$$\text{Drug} - \text{loading} = \frac{C \times V}{M \times 10^6} \times 100\% \quad (2)$$

where C (μg/ml) is the myricetin concentration in the supernatant, V (ml) is the volume of the supernatant, m (g) is the total mass of the added myricetin, M (g) is the total mass of the added myricetin plus casein.

2.5 Characterisation of casein–myricetin nanomicelles

The UV–visible (vis) absorption spectroscopy experiments were carried out with UV-752. Absorption spectra were recorded for casein–myricetin nanomicelles, myricetin solution, and casein solution over the range of 200–600 nm, respectively. Casein, myricetin, and casein–myricetin nanomicelles samples were also identified by Fourier transform infrared (FTIR) spectroscopy. The microstructure of the casein–myricetin nanomicelles was observed by transmission electron microscopy (TEM). The samples to be tested were measured for polydispersity (PDI), particle size, and zeta by zetasizer Nano S90 (Malvern Instruments Ltd, UK) after dilution with water.

2.6 Determination of the critical micelle concentration (CMC) of casein micelles

Aliquots of pyrene solution (10×10^{-7} M in acetone) were added to various concentrations of casein micelles, followed by sonication for 5 min. After evaporated to remove acetone and recorded fluorescence spectra using an F-2700 spectrofluorophotometer (HITACHI, Japan). The excitation fluorescence spectrum and emission fluorescence wavelength were set as 330–374 and 385 nm. The intensity ratio of the peak at 374 nm (I1) and 385 nm (I3) was calculated and plotted against the logarithm of casein micelles concentration [31].

2.7 Optimisation of casein nanoparticles self-assembly conditions

The influence of different pH (2.5–7.0, interval 0.5) and casein concentration (1–6 mg/ml of six groups) on the particle size and dispersion coefficient of nanoparticles were studied under other fixed conditions.

2.8 Optimisation of preparation conditions of casein–myricetin nanomicelles

The encapsulation yield and drug loading were further improved by optimising the four variables, myricetin dosage (the mass ratio of casein and myricetin ranges from 4 to 12), ultrasonic power (200–400 W), ultrasonic time (2–20 min) and the amount of ethanol (5–11 ml).

2.9 Closed-loop rat intestinal perfusion

The in situ closed-loop intestinal perfusions followed previously published reports [32]. Male SD rats (180–220 g) were fasted for 12 h with free access to water before the perfusion experiment. Rats were anesthetised with 10% chloral hydrate (3 ml/kg) injection and placed on a heated surface to maintain normal body temperature. A midline abdominal incision was made, and the small intestine was exposed. Intubation and ligation after incision at both ends of the upper part of the duodenum and the lower part of the ileum. Rinsed with 37°C saline and Krebs–Ringer phosphate buffer solution. The catheters were connected to a constant-flow pump to form a loop. The test solution was perfused at 37°C through the intestinal lumen at a constant flow rate of 5 ml/min. This solution was first perfused for 10 min to ensure a steady state [33]. After a steady state, then the flow rate adjusted to 3 ml/min. Samples collected at 0, 15, 30, 60, 80, 100, and 120 min were analysed by HPLC. Adding an equal volume of 37°C Krebs–Ringer phosphate buffer solution after each sampling and the cycle was stopped after sampling seven times. Finally, animals were sacrificed according to protocols for euthanasia in experimental animals [34, 35].

2.10 Method validation

Specificity was evaluated by analysing the concentration of analytes in blank intestinal perfusion solution to investigate the potential interferences of intestinal perfusate endogenous to the analytes. Myricetin (2 mg) and 200 mg/l of PSP (6 mL) were mixed, and diluted to 60 ml with blank intestinal circulation solution, place in a constant temperature water bath at 37°C for 2 h and determine myricetin concentration at 0,1, and 2 h.

2.11 Ethics statement

Animal experiments were carried out in strict accordance with the National Institute of Health Guidelines on the ethical use of animals. All surgeries were operated under chloral hydrate, and every effort was made to minimise suffering.

2.12 Statistical analysis

All experiments contained three rats per perfusion group. The results were presented as mean. Data and graphs are analysed using origin 9.0 software.

3 Results and discussion

3.1 UV absorption experiment

UV–vis absorption spectra can be used for predicting the drug molecules–casein complex formation [25]. Fig. 1 shows that myricetin has characteristic absorption peaks of flavonoids at 254 and 376 nm. Casein has two absorption peaks at 228 and 278 nm. The casein–myricetin nanomicelles showed two absorption peaks at 259 and 372 nm. The peak of myricetin is bathochromic shifted, and the hypochromic shift of casein peak indicates that the microenvironment of tyrosine residue has changed.

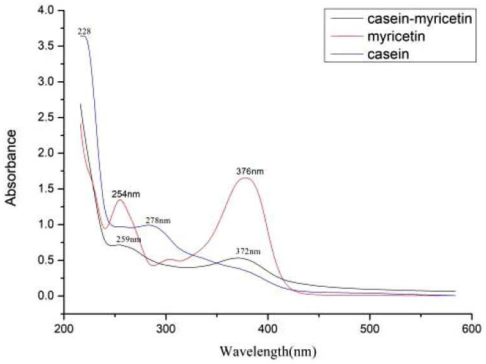

Fig. 1 *UV absorption spectrum of casein–myricetin, myricetin, and casein*

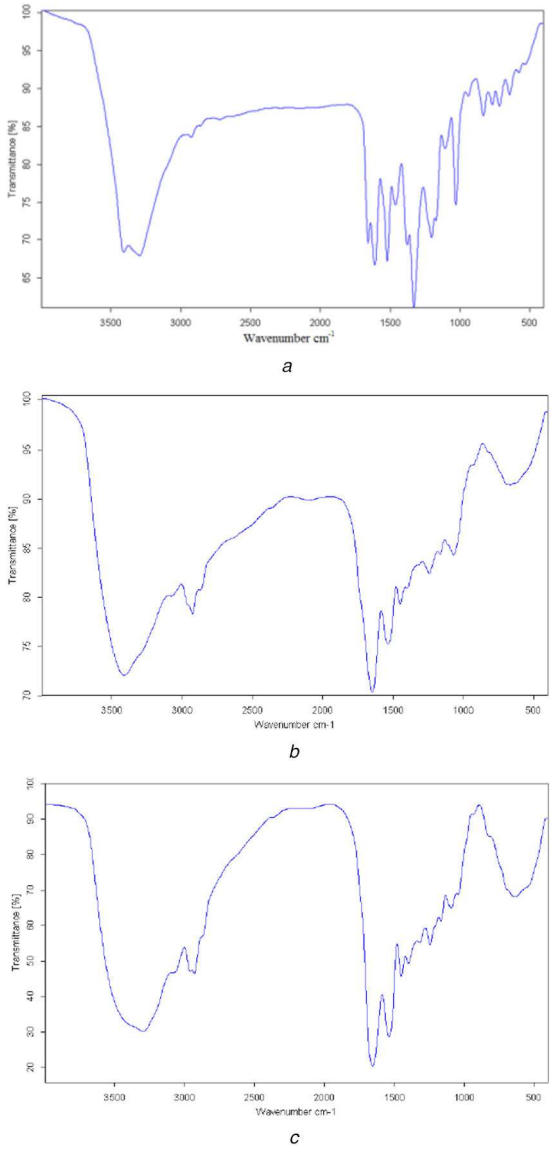

Fig. 2 *Infrared absorption spectrum*
(a) Myricetin, ***(b)*** *Casein*, ***(c)*** Casein–myricetin nanomicelles

3.2 Infrared spectrum

The structural changes in the myricetin and casein were also examined by FTIR spectroscopy. As shown in Fig. 2, The infrared spectrum of casein–myricetin is almost identical to that of casein, however, many of the characteristic peaks of myricetin are decreased or disappeared. The amino peak at 3301 cm^{-1} in Fig. 2*c* the amides peak at 1648 cm^{-1}, the carbonyl peak at 1671 cm^{-1} of myricetin disappeared, and the stretching vibration of the benzene ring skeleton at 1450 and 1606 cm^{-1} disappeared. A series of changes in the FTIR spectrum indicates that myricetin is encapsulated in casein after self-assembly because FTIR can only detect the infrared absorption of surface substances.

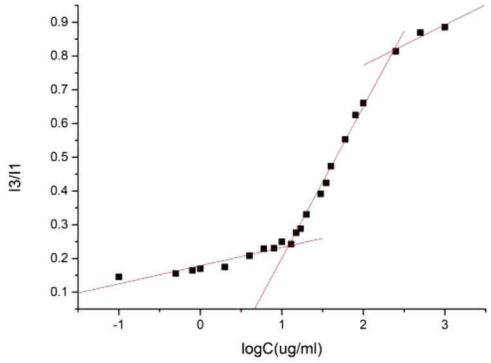

Fig. 3 *Relationship of the intensity ratio (I3/I1) and the concentration of casein micelles*

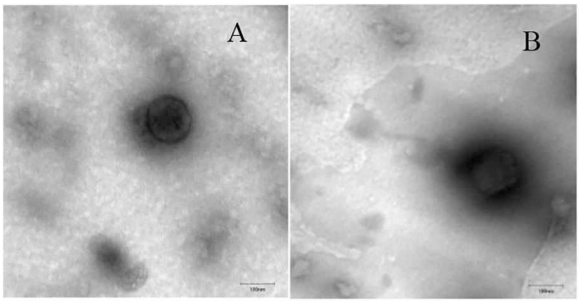

Fig. 4 *TEM images of nanomicelles*
(a) Casein nanomicelles, ***(b)*** Casein–myricetin nanomicelles

3.3 CMC of casein micelles

The pyrene probe fluorescence spectrometry is a recognised method to determine the CMC value. The emission intensity ratio of I3/I1 is affected by the polarity of the medium surrounding pyrene molecules. The relationship of the I3/I1 and the concentration of casein micelles are shown in Fig. 3. At low concentration, the intensity ratio of I3/I1 remained nearly unchanged. As the concentration increases, the intensity ratio of I3/I1 starts to increase dramatically and reaches the characteristic level of pyrene in completely hydrophobic environments at a certain concentration of casein micelles. The CMC of the amphiphilic casein micelles obtained from the curve was 11.99 μg/ml.

3.4 TEM analysis

TEM images provide evidence of casein micelles formation. As shown in Fig. 4, casein micelles have a spherical structure with a particle size of 140 nm. There was no significant difference in the appearances of the myricetin-free micelles and the myricetin-loaded micelles.

3.5 Optimisation of self-assembly conditions of casein nanomicelles

The pH and casein concentration has a great influence on the particle size and dispersion coefficient. Therefore, these two factors are selected to optimise the self-assembly conditions of the casein nanomicelles. The average particle size of the casein micelles in milk is about 150 nm. The aim of this study was to reduce the size of the prepared micelles and approach to this value so that the self-assembly products can play a better role.

Protein solubility is related to system pH. When the pH deviates from the isoelectric, the casein molecules have more net charge, and the electrostatic repulsion between the molecules is stronger, resulting in a loose structure and larger particle size. When the pH was <3.5, the particle size and PDI decreased with the raise of pH,

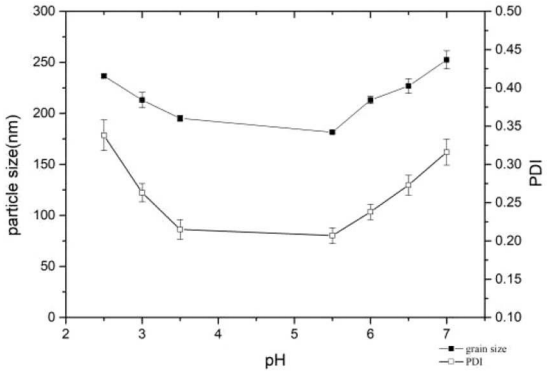

Fig. 5 *Changes of particle size and PDI of casein–myricetin nanomicelles at different pH*

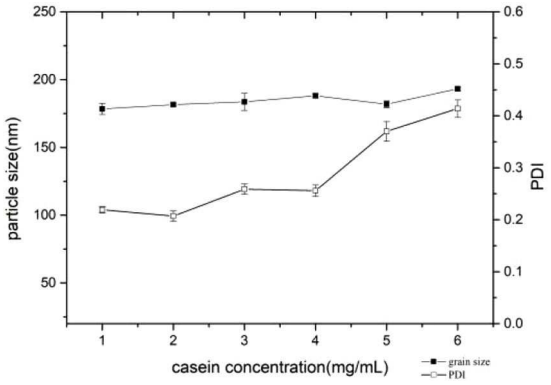

Fig. 6 *Changes of particle size and PDI of casein–myricetin nanomicelles at different casein concentrations*

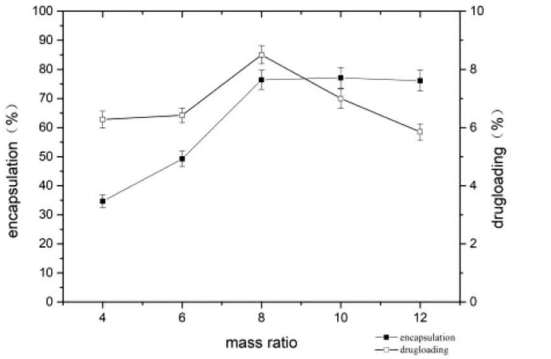

Fig. 7 *Changes of encapsulation yield and drug loading of casein–myricetin nanomicelles at different mass ratios*

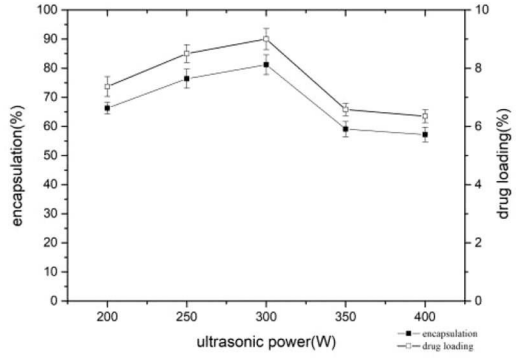

Fig. 8 *Changes of encapsulation yield and drug loading of casein–myricetin nanomicelles at different ultrasonic power*

reaching the minimum value of 5.5, which were 181.60 ± 1.10 and 0.207± 0.010 nm. A gradual increase in the PDI and particle size was observed with increasing pH when the pH is in the range of 5.5–7.0 (Fig. 5). When the pH is changed within the range of 3.5–5.5, which is close to the isoelectric point (pH = 4.7). The molecules collide with each other and start to precipitate. At this time, ultrasonication cannot uniformly disperse the insoluble casein. Therefore, the particle size cannot be measured accurately. A lower PDI means a higher uniform distribution.

The concentration of casein can affect the state of particle aggregation. It can be seen from Fig. 6 that the minimum PDI was observed at 2 mg/ml when the casein concentration varied from 1 to 6 mg/ml. However, the particle size did not change significantly and floated substantially in the range of 180–190 nm. It indicated that the particle size distribution of the self-assembled nanoparticles is the narrowest at this concentration, and the nanoparticles in the system are the most homogeneous and stable.

3.6 Optimisation of preparation conditions of casein–myricetin nanomicelles

The mass ratio of casein to myricetin has a great impact on the encapsulation yield and drug loading of self-assembled nanomicelles. It can be seen from Fig. 7 that as the mass ratio of casein to myricetin increases, the encapsulation yield increases. Also, when the mass ratio reaches 8:1, the encapsulation yield hardly changes, showing a stable trend. However, the drug loading increased first and then decreased with the increase of casein and myricetin mass ratio, and the maximum was observed at 8:1. Within a certain range, an increase of casein and myricetin mass ratio helps to form a greater number of casein particle aggregates in the system. At low concentration of casein, casein micelles appear to behave like solid spheres and the hydrophobic interaction between the casein and myricetin was utilised for the encapsulation. However, casein micelles at high concentrations of casein act as a soft sphere that deforms in the direction of shear stress. The deformation makes the casein particles less potent to encapsulate myricetin [36]. Furthermore, the result indicates that the available attractive sites of casein particles for the encapsulation got saturated by the casein and myricetin mass ratio of 8:1.

With the increase of ultrasonic power, the encapsulation yield and the drug loading both increased first and then decreased. When the ultrasonic power is 300 W, the encapsulation yield and the drug loading are maximum, were 81.20 ± 3.41 and 9.00 ± 0.36%, respectively (Fig. 8). Within a certain range, due to the increase of power, the shear force and pressure caused by the cavitation effect will cause the violent collision of particles. Also, the constant impact destroys the irregular protein structure that initially scattered on the surface of the particle. Finally, the particle shape is distributed regularly, the self-assembly system is more uniform, and both the drug loading and encapsulation yield have improved.

The encapsulation yield and drug loading of nanomicelles under different ultrasound times are shown in Fig. 9. With the extension of ultrasound time, the encapsulation yield and drug loading both showed a trend of increasing first and then decreasing. It reaches the maximum at 5 min. The prolonging of the ultrasonic time accelerates the self-assembly between the molecules in a short time; however, the ultrasonic time is too long that destroys the self-assembled nanomicelles, resulting in the re-release of myricetin embedded in the complex.

As can be seen from Fig. 10, the encapsulation yield and drug loading reach the maximum at 7 ml of ethanol. With the increase of ethanol amount, the dispersion and solubility of myricetin in the ethanol–water system increased, and the probability of self-assembly of myricetin and casein solution increased, so the encapsulation yield and the drug loading increased too. However, the excessive amount of ethanol will change the spatial structure of casein and expose the hydrophobic groups that were originally buried inside. The water solubility of the casein protein nanoparticle is affected and the self-assembly process is further carried out, resulting in the decrease of the encapsulation yield and drug loading.

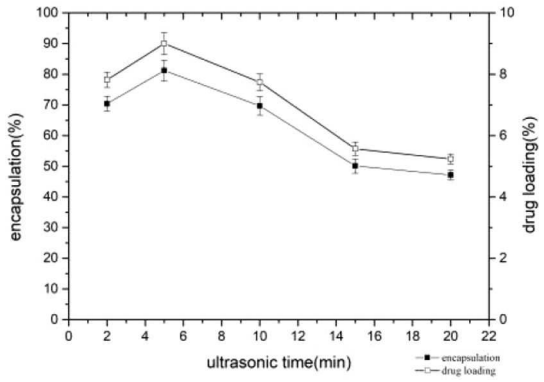

Fig. 9 *Changes of encapsulation yield and drug loading of casein–myricetin nanomicelles at different ultrasonic times*

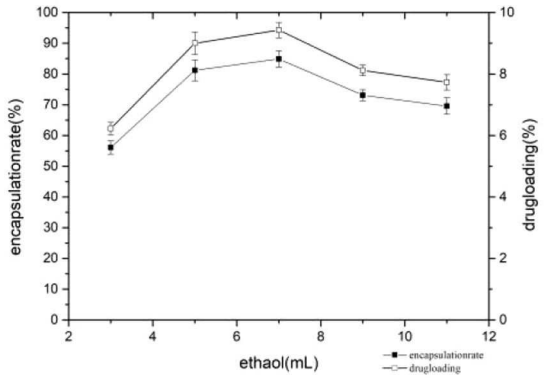

Fig. 10 *Changes of encapsulation yield and drug loading at different ratios of ethanol consumption*

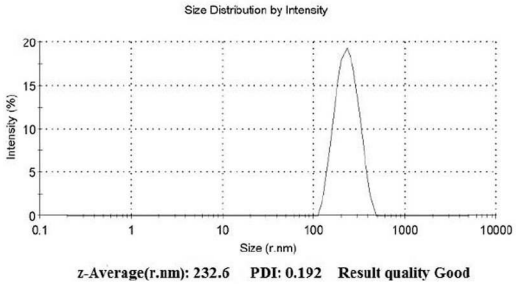

Fig. 11 *Casein–myricetin nanomicelles size and dispersion coefficient*

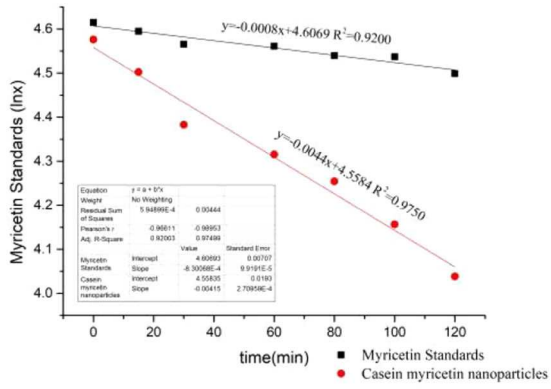

Fig. 12 *Myricetin standard sample and casein–myricetin nanomicelles in rat small intestine 2 h absorption (n = 7)*

3.7 Determination of particle size and zeta

The casein–myricetin nanomicelles were prepared under the optimum conditions (casein concentration 2 mg/ml, pH 5.5, the mass ratio of casein to myricetin 8:1, ultrasonic power 300 W, ultrasonic time 5 min, ethanol addition 7 ml) for self-assembly. The size and dispersion coefficient were determined. The results were 232.6 nm and 0.192, respectively (Fig. 11). The particle size measured by dynamic light scattering (DLS) was larger than those estimated by TEM, and this phenomenon can be attributed to the aggregation of micelles or higher-order assemblies. Furthermore, the sample had been diluted during the staining process, and most of the aggregates of micelles or higher-order assemblies may dissociate and may not be observed by TEM [37]. The casein–myricetin nanomicelles have a zeta potential of−6.65±0.11 mV.

Table 1 Absorption results of myricetin standards and casein–myricetin nanomicelles in rat small intestine during 2 h

Sample	Absorption rate constant, K_a	Absorption rate, %
myricetin standard sample	8.0×10^{-4}	10.90
casein–myricetin nanomicelles	4.4×10^{-3}	.60

3.8 Method validation

Blank intestinal circulation with myricetin was placed in a water bath at 37°C. The concentration of myricetin increased by (0.36 ± 0.27)% after 1 h, and increased by (0.45 ± 0.33)% at 2 h compared with 0 h, which may be due to the increase of myricetin solubility over time. Therefore, it is considered that myricetin can stably exist for 2 h in the blank intestinal circulatory fluid and will not interfere with the measurement results of intestinal absorption experiments.

3.9 Closed-loop rat intestinal perfusion

The standard curves of PSP and myricetin were drawn and corrected the volume of the test solution by the PSP. Finally, the residual amount of myricetin in the test solution was calculated. The absorption of casein–myricetin nanomicelles in the small intestine is significantly better than myricetin (Fig. 12). The absorption rates of nanomicelles are significantly higher than that of myricetin (Table 1).

In conclusion, self-assembly using amphiphilic materials as carriers is widely used in the pharmaceutical, food, and chemical industries and is capable of trapping hydrophobic pharmaceuticals and active ingredients in the core. This characteristic increases the stability, solubility, and bioavailability of such trapped ingredients [38–40]. Amphiphilic materials can also be used as carriers for sustained release agents to prolong the action time of drugs in the body. In this study, casein–myricetin nanomicelles were successfully prepared by self-assembly, and the optimal conditions for preparation of casein–myricetin nanomicelles were investigated. The casein concentration was 2 mg/ml, pH 5.5, and casein and myricetin. The ratio of 8:1, ultrasound power 300 W, ultrasound time 5 min, the amount of ethanol added 7 ml. The absorption of casein–myricetin nanomicelles in rats was detected by intestine perfusion in rats. The absorption rate of prepared nanomicelles was four times that of myricetin standards. The results of this study provide the possibility of preparing myricetin in oral preparations.

4 Acknowledgments

This work was financially supported by the Zhejiang Provincial Natural Science Foundation of China under grant no. LY16C020005.

5 References

[1] Siegelin, M.D., Gaiser, T., Habel, A., *et al.*: 'Myricetin sensitizes malignant glioma cells to trail-mediated apoptosis by down-regulation of the short isoform of flip and bcl-2', *Cancer Lett.*, 2009, **283**, (2), pp. 230–238

[2] Shimmyo, Y., Kihara, T., Akaike, A., *et al.*: 'Three distinct neuroprotective functions of myricetin against glutamate-induced neuronal cell death: involvement of direct inhibition of caspase-3', *J. Neurosci. Res.*, 2008, **86**, (8), pp. 1836–1845

[3] Zhang, Q., Zhao, X.H., Wang, Z.J.: 'Flavones and flavonols exert cytotoxic effects on a human oesophageal adenocarcinoma cell line (oe33) by causing g2/m arrest and inducing apoptosis', *Food Chem. Toxicol.*, 2008, **46**, (6), pp. 2042–2053

[4] Kan, X., Liu, B., Guo, W., *et al.*: 'Myricetin relieves LPS-induced mastitis by inhibiting inflammatory response and repairing the blood–milk barrier', *J. Cell. Physiol.*, 2019, **234**, pp. 16252–16262

[5] Lin, G.B., Xie, Y., Li, G.W.: 'Progress in the study of myricetin', *J. Int. Pharm. Res.*, 2012, **39**, (6), pp. 483–487

[6] Lin, S.Y., Gao, J.G., Guo, Q.Q.: 'The stability of dihydromyricetin and its influencing factors', *J. Wuxi Univ. Light Ind.*, 2004, **23**, (2), pp. 17–20

[7] Guo, R.X., Fu, X., Chen, J., *et al.*: 'Preparation and characterization of microemulsions of myricetin for improving its antiproliferative and antioxidative activities and oral bioavailability', *J. Agric. Food Chem.*, 2016, **64**, (32), pp. 6286–6294

[8] Landi-Librandi, A. P., de Oliveira, C. A., Azzolini, A. E.: 'In vitro evaluation of the antioxidant activity of liposomal flavonols by the HRP-H2O2-luminol system', *J. Microencapsul.,* 2011, **28**, (4), pp. 258–267.

[9] Zhang, Y.H., Wang, S.J., Xu, K., *et al.*: 'Preparation and quality evaluation of myricetin microemulsion', *J. Shenyang Pharm. Univ.*, 2010, **27**, (10), pp. 777–783

[10] Yao, Y.S., Xie, Y., Hong, C., *et al.*: 'Development of a myricetin/hydroxypropyl-β-cyclodextrin inclusion complex: preparation, characterization, and evaluation', *Carbohydr. Polym.*, 2014, **110**, pp. 329–337

[11] Mehranfar, F., Bordbar, A.K., Parastar, H.: 'A combined spectroscopic, molecular docking and molecular dynamic simulation study on the interaction of quercetin with β-casein nanoparticles', *J. Photochem. Photobiol. B*, 2013, **127**, (10), pp. 100–107

[12] Xiao, J., Kai, G., Yang, F., *et al.*: 'Molecular structure-affinity relationship of natural polyphenols for bovine gamma-globulin', *Mol. Nutr. Food Res.*, 2011, **55**, pp. 86–92

[13] Xiao, J.B., Kai, G.A.: 'Review of dietary polyphenol-plasma protein interactions: characterisation, influence on the bioactivity, and structure–affinity relationship', *Crit. Rev. Food Sci.*, 2012, **52**, (1), pp. 85–101

[14] Xiao, J.B., Chen, T.T., Cao, H.: 'Molecular property–affinity relationship of flavanoids and flavonoids for human serum albumin in vitro', *Mol. Nutr. Food Res.*, 2011, **55**, (2), pp. 310–317

[15] Ball, P.: 'Materials science: polymers made to measure', *Nature*, 1994, **367**, pp. 323–324

[16] Whitesides, G.M., Mathias, J.P., Seto, C.T.: 'Molecular self-assembly and nanochemistry: a chemical strategy for the synthesis of nanostructures', *Science*, 1991, **254**, pp. 1312–1319

[17] Yu, B., Bian, H., Plank, J.: 'Self-assembly and characterization of CA–AL–LDH nanohybrids containing casein proteins as guest anions', *J. Phys. Chem. Solids*, 2010, **71**, (4), pp. 468–472

[18] Farías, M. E., Martinez, M. J., Pilosof, A. M. R.: 'Casein glycomacropeptide pH-dependent self-assembly and cold gelation', *Int. Dairy J.*, 2010, **20**, (2), pp. 79–88.

[19] Setter, O., Livney, Y.D.: 'The effect of sugar stereochemistry on protein self-assembly: the case of beta-casein micellization in different aldohexose solutions', *Phys. Chem. Chem. Phys.*, 2015, **17**, (5), pp. 3599–3606

[20] Yu, J., Liu, C.G.: 'Review of research on edible proteins as nutrient carriers', *Sci. Technol. Food Ind.*, 2012, **4**, pp. 438–441

[21] Głąb, T.K., Boratyński, J.: 'Potential of casein as a carrier for biologically active agents', *Top. Curr. Chem.*, 2017, **375**, p. 71

[22] Dalgleish, D.G.: 'On the structural models of bovine casein micelles-review and possible improvements', *Soft Mat.*, 2011, **7**, (6), pp. 2265–2272

[23] Xue, J., Tan, C., Zhang, X., *et al.*: 'Fabrication of epigallocatechin-3-gallate nanocarrier based on glycosylated casein: stability and interaction mechanism', *J. Agric. Food Chem.*, 2014, **62**, (20), pp. 4677–4684

[24] Debika, G., Regupathi, I.: 'Selective encapsulation of quercetin from dry onion peel crude extract in reassembled casein particles', *Food Bioprod. Process.*, 2011, **115**, pp. 100–109

[25] Cao, X.Y., He, Y.L., Kong, Y.C., *et al.*: 'Elucidating the interaction mechanism of eriocitrin with β-casein by multispectroscopic and molecular simulation methods', *Food Hydrocolloids*, 2019, **94**, pp. 63–70

[26] Liu, L. L., Liu, P. Z., Li, X. T., *et al.*: 'Novel soy β-conglycinin core–shell nanoparticles as outstanding ecofriendly nanocarriers for curcumin', *J. Agric. Food Chem.*, 2019, **67**, pp. 6292–6301

[27] Liu, Q.G., Jing, Y.Q., Han, C.P.: 'Encapsulation of curcumin in zein/caseinate/sodium alginate nanoparticles with improved physicochemical and controlled release properties', *Food Hydrocolloids*, 2019, **93**, pp. 432–442

[28] Awadeen, R.H., Boughdady, M.F., Meshali, M.M.: 'New in-situ gelling biopolymer-based matrix for bioavailability enhancement of glimepiride, in-vitro/in-vivo X-ray imaging and pharmacodynamic evaluations', *Pharm. Dev. Technol.*, 2019, **24**, (5), pp. 539–549

[29] Zheng, Y. F., Xiao, L. Z., Yu, C. H., *et al.*: 'Enhance antiarthritic efficacy by nanoparticles of (−)-epigallocatechin gallate glucosamine–casein', *J. Agric. Food Chem.*, 2019, **67**, pp. 6476–6486.

[30] Henrike, M., Dierk, M., Katrin, S., *et al.*: 'Spray- or freeze-drying of casein micelles loaded with vitamin D2: studies on storage stability and in vitro digestibility', *LWT*, 2018, **97**, pp. 87–93

[31] Liu, J., Pang, Y., Huang, W.: 'Self-assembly of phospholipid-analogous hyperbranched polymers nanomicelles for drug delivery', *Biomaterials*, 2010, **31**, (6), pp. 1334–1341

[32] Doluisio, J. T., Billups, N. F., Dittert, L.W., *et al.*: 'Drug absorption: I. An in situ rat gut technique yielding realistic absorption rates', *J. Pharm. Sci.,* 1969, **58**, pp. 1196–1200.

[33] Reis, J.M., Dezsni, A.B., Pereira, T.M., *et al.*: 'Lamivudine permeability study: a comparison between PAMPA, ex vivo and in situ single-pass intestinal perfusion (SPIP) in rat jejunum', *Eur. J. Pharm. Sci.*, 2013, **48**, pp. 781–789

[34] VMA: 'A VMA guidelines on euthanasia: formerly reported of the A VMA panel on euthanasia', [M] Lu, X.C.J. Beijing: People's Medical Publishing House, 2019, pp. 51–54

[35] Sutton, S.C., Rinaldi, M.T., Vukovinsky, K.E.: 'Comparison of the gravimetric, phenol red, and 14C-PEG-3350 methods to determine water absorption in the rat single-pass intestinal perfusion model', *AAPS Pharm. Sci.*, 2001, **3**, (3), p. 93

[36] Visina, A.: 'Characterization of casein micelles and sodium caseinate in dense suspensions'. Master thesis, Lund University, Sweden, 2016.

[37] Liu, Q.Q., Liang, R., Zhong, F., *et al.*: 'Self-assembled micelles based on OSA-modified starches for enhancing solubility of β-carotene: effect of starch macromolecular architecture', *J. Agric. Food Chem.*, 2019, **67**, pp. 6614–6624

[38] Nishiura, H., Sugimoto, K., Akiyama, K., *et al.*: 'A novel nano-capsule of α-lipoic acid as a template of core-shell structure constructed by self-assembly', *Nanomed. Nanotechnol.*, 2013, **4**, pp. 155–161

[39] Bisht, S., Feldmann, G., Soni, S., *et al.*: 'Polymeric nanoparticle-encapsulated curcumin ('nanocurcumin'): a novel strategy for human cancer therapy', *J. Nanobiotechnol.*, 2007, **5**, pp. 1–18

[40] Thi, T., La, T.H., Le, T.P., *et al.*: 'Docetaxel and curcumin-containing poly(ethylene glycol)-block-poly-(ε-caprolactone) polymer micelles', *Adv. Nat. Sci.-Nanosci.*, 2013, **4**, (2), p. 025006